
000 STEERING VECTOR TRANSFER VIA ORTHONORMAL 001 002 TRANSFORMATIONS AND SEMANTIC PAIRING 003 004

005 **Anonymous authors**

006 Paper under double-blind review

009 ABSTRACT 010

011 Steering vectors—directions in activation space encoding behavioral traits
012 like formality or creativity—enable fine-grained control over language model
013 outputs but must be regenerated for each new model, creating deployment
014 barriers. We present a method for transferring these vectors between dif-
015 ferent language models by learning structure-preserving transformations
016 while matching corresponding text pairs across models. Our approach
017 achieves strong alignment (0.50-0.56 cosine similarity, where 1.0 represents
018 perfect alignment and 0.0 represents random chance) across all model pairs
019 tested. Crucially, we demonstrate that semantic pairing—ensuring each text
020 contrast is matched across models during training—improves transfer per-
021 formance by 72%: proper pairing achieves 0.529 cosine similarity compared
022 to 0.308 with shuffled pairs within traits and 0.00 with random pairing
023 across traits. We evaluate our method across 26 behavioral traits on three
024 architecturally distinct models (Gemma-7B, LLaMA-3-8B, and Mistral-7B),
025 using dimensionality reduction to handle their different hidden dimensions.
026 Our results provide evidence for the Platonic Representation Hypothesis,
027 showing that different language models encode behavioral preferences in
028 similar geometric structures. This enables practical reuse of curated steering
029 vectors across model families and advances our understanding of how neural
030 networks represent human preferences.

031 1 INTRODUCTION 032

033 This work addresses the challenge of reusing behavioral control mechanisms across different
034 language models. We develop a novel method to transfer steering vectors across diverse
035 model families, enabling the reuse of curated behavioral controls without regeneration. This
036 capability addresses critical deployment barriers: organizations cannot maintain reusable
037 steering libraries, researchers need generation access to study behaviors, and computational
038 resources are wasted regenerating identical controls. Steering vectors—directions in activation
039 space learned from pairs of contrasting behaviors—provide precise control over language
040 model outputs without retraining Turner et al. (2023); Zou et al. (2023). These vectors are
041 extracted by computing activation differences between contrasting behaviors (e.g., formal vs.
042 informal text) and operate through activation engineering without modifying model weights.
043 However, they remain applicable only within individual models: a formality vector extracted
044 from GPT-4 cannot be used to steer LLaMA-3, requiring new vectors to be regenerated
045 for every new model deployment. These limitations arise from architectural differences
046 including different hidden dimensions (e.g., 3072 for Gemma-7B-Instruct versus 4096 for
047 LLaMA-3-8B-Instruct), attention mechanisms, and learned representations.

048 Our goal is to understand if different language models encode behavioral traits in similar
049 linear subspaces. We approach this problem by identifying orthogonal transformations
050 between paired steering vectors across different models, using geometric alignment (structure-
051 preserving transformations) and semantic pairing (matching identical text contrasts across
052 models). The degree of representational universality—how much different models share
053 similar representations for behavioral traits—remains an open question in neural network
research.

054 Three key applications emerge from successful steering vector transfer: (1) *Large-scale*
055 *curation*: Libraries containing thousands of steering vectors can be transferred to new models
056 in under 10 minutes, compared to days or weeks of regeneration from scratch. (2) *Data-*
057 *restricted domains*: Organizations can generate vectors once on secure systems with sensitive
058 data, then transfer them to deployment models without retaining the original training data.
059 (3) *Model-restricted research*: Researchers can study behavioral controls in closed commercial
060 systems by transferring vectors from open-source alternatives.

061 Surprisingly, our investigation reveals that despite substantial architectural differences,
062 instruction-tuned models (Mistral-7B-Instruct Jiang et al. (2023), Gemma-7B-Instruct
063 Gemma Team et al. (2024), and Llama-3-8B-Instruct Dubey et al. (2024)) exhibit significant
064 representational universality: they encode preference traits in alignable linear subspaces.
065 This finding provides empirical evidence for the Platonic Representation Hypothesis Huh et al.
066 (2024), demonstrating that neural networks converge to shared representations specifically
067 in the domain of behavioral traits. Our work operationalizes this hypothesis by quanti-
068 fying the degree of alignment and showing that LLMs encode preferences in structured,
069 linearly-alignable representations despite their architectural diversity. Crucially, we find
070 that preserving relationships between vectors—not just individual vectors—is essential for
071 successful transfer.

072 Our contributions are:

073

- 074 1. We develop a novel method for cross-model steering vector transfer that preserves
075 geometric structure through orthogonal transformations and scaling, maintaining
076 relationships between vectors.
- 077 2. We demonstrate that matching text contrasts across models (semantic pairing)
078 improves transfer performance by 77% (from 0.30 to 0.529 cosine similarity).
- 079 3. We validate our method across 26 behavioral traits and 3 model families, revealing
080 that objective linguistic traits transfer well (>0.55 cosine similarity) while subjective
081 traits transfer poorly (<0.45 cosine similarity).

082 The success of linear alignment with semantic pairing opens new research directions for
083 understanding the geometric structure of preference representations and developing universal
084 behavioral control interfaces across model families. Our evaluation focuses on geometric
085 alignment metrics rather than downstream behavioral validation, which we leave for future
086 work.

088 2 RELATED WORK

089 **Steering Vectors.** Steering vectors, introduced by Turner et al. (2023) as Activation
090 Addition, enable fine-grained control over model behavior without optimization. Zou et al.
091 (2023) extend this with Representation Engineering, demonstrating behavioral control across
092 multiple dimensions. Ardiit et al. (2024) show that refusal is mediated by a single direction,
093 while Liu et al. (2024) demonstrate in-context steering. All these approaches remain model-
094 specific. Our work enables transfer across model families, making steering vectors practical
095 for multi-model deployments.

096 **Representation Alignment Methods.** Prior work has developed various approaches
097 for comparing and aligning neural representations. Kornblith et al. (2019) and Raghu
098 et al. (2017) provide metrics for measuring representational similarity but do not enable
099 practical transfer between models. Model stitching Bansal et al. (2021) connects layers
100 across models but requires matching architectures (e.g., ResNet-50 to ResNet-101), not
101 diverse model families with different attention mechanisms and dimensions like Gemma
102 to LLaMA. Domain adaptation literature has explored geometric approaches including
103 Grassmann manifolds Gong et al. (2012) and matrix manifold optimization Absil et al. (2008)
104 for representation alignment. The Platonic Representation Hypothesis Huh et al. (2024)
105 provides theoretical motivation, suggesting models converge to shared representations. While
106 prior work focused primarily on mathematical frameworks for alignment, we demonstrate
107 that preserving the correspondence between specific text contrasts across models is equally

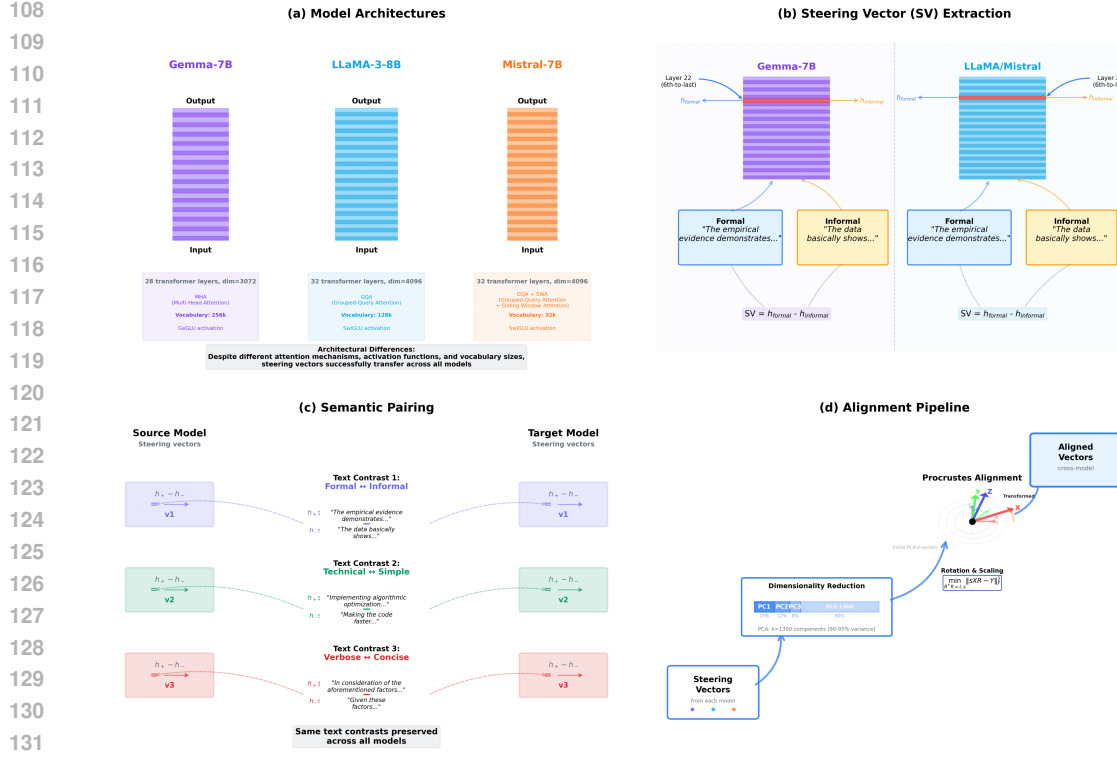


Figure 1: **Steering vector transfer via semantic pairing.** (a) Three model architectures with varying dimensions and attention mechanisms. (b) Steering vector extraction from contrasting trait text pairs at the sixth-to-last layer, computed as normalized differences between positive and negative trait examples. (c) Semantic pairing preserves instance-level correspondence by ensuring the same text contrast pairs are matched across models during alignment. (d) Procrustes alignment pipeline using PCA reduction followed by whitening and orthogonal rotation to learn structure-preserving transformations.

important for successful behavioral transfer. Our use of Procrustes analysis Schönemann (1966); Gower (1975) provides both theoretical grounding through its optimality properties and practical efficiency.

3 PRELIMINARIES

3.1 BEHAVIORAL TRAITS

In our framework, a *trait* represents a measurable behavioral or stylistic dimension along which text can vary. Each trait is defined through contrastive text pairs that exemplify opposite ends of the dimension—for instance, formal vs. informal writing style, verbose vs. concise expression, or assertive vs. passive tone. We study 26 traits spanning linguistic properties (e.g., formality, clarity, specificity), emotional dimensions (e.g., optimism, empathy, enthusiasm), and communicative styles (e.g., directness, persuasiveness, authority). These traits are operationalized through 65,329 human-curated or naturally-occurring text pairs that demonstrate clear contrasts along each dimension.

3.2 PROBLEM FORMULATION

Given these behavioral traits, our approach enables transfer when models encode similar semantic structure despite architectural differences. Let $\mathcal{V}_s^{(i)} \in \mathbb{R}^{d_s}$ and $\mathcal{V}_t^{(i)} \in \mathbb{R}^{d_t}$ denote steering vectors for trait i in source and target models respectively, where d_s and d_t are

162 the hidden dimensions. Our goal is to learn an orthonormal transformation $R \in SO(d)$
163 (specifically a rotation matrix) and scale factor $s \in \mathbb{R}^+$ that enable transfer:
164

$$165 \quad \mathcal{V}_t^{(i)} \approx T(\mathcal{V}_s^{(i)}) = s \cdot R(\mathcal{V}_s^{(i)}) \quad (1)$$

166 where the rotation matrix R preserves geometric structure (angles and relative distances)
167 and the scale factor s accounts for differences in activation magnitudes between models,
168 which arise from varying initialization schemes, training dynamics, and normalization layers.
169

170 Orthogonal transformations preserve angles and relative distances, ensuring meaningful
171 alignments that reflect true structural similarities rather than arbitrary mappings Kornblith
172 et al. (2019). Following prior work that uses PCA projection to identify relevant subspaces
173 before alignment Raghu et al. (2017), we first reduce dimensionality to concentrate trait-
174 relevant information. This approach builds on methods like SVCCA Raghu et al. (2017) and
175 CKA Kornblith et al. (2019) that analyze neural network representations, though our focus
176 is on enabling practical transfer rather than measurement alone. The complete alignment
177 pipeline, including PCA projection and Procrustes analysis, is detailed in Section 3.
178

179 4 METHOD

180 We present our approach for transferring steering vectors across language models through
181 linear geometric alignment with semantic pairing. Steering vectors encode behavioral traits
182 as directions in activation space. For each contrast pair (t^+, t^-) representing positive
183 and negative examples of a trait, we encode both texts through each model and extract
184 hidden states from intermediate layers. The steering vector is computed as the normalized
185 difference between these hidden states: $v = \frac{h(t^+) - h(t^-)}{\|h(t^+) - h(t^-)\|_2}$, where $h(\cdot)$ denotes the hidden
186 state extraction function. This normalization ensures that all steering vectors have unit
187 magnitude, facilitating comparison across different traits and models.
188

189 Our method achieves cross-model steering vector transfer through three key modules: (1)
190 PCA projection to identify trait-relevant subspaces where information is concentrated, (2)
191 Procrustes alignment to learn orthogonal transformations that preserve geometric structure,
192 and (3) semantic pairing to maintain instance-level correspondence.
193

194 4.1 STEERING VECTOR TRANSPORT

195 To concentrate trait-relevant information, we first project steering vectors to a lower-
196 dimensional subspace. For each model, we first collect steering vectors across all 26 traits:
197 $\{\mathcal{V}^{(1)}, \dots, \mathcal{V}^{(26)}\}$. We then apply global mean-centering (across all traits) to remove the
198 average activation pattern, apply PCA to identify the top- k principal components, and
199 project vectors to this k -dimensional subspace.
200

201 We choose k to capture sufficient variance while maintaining computational efficiency. Im-
202 portantly, we use PCA *without whitening* to preserve the relative scale of variations along
203 different principal components.
204

205 We use Procrustes alignment Schönemann (1966); Gower (1975) to learn orthogonal trans-
206 formations that preserve geometric structure. Given projected source vectors $X \in \mathbb{R}^{n \times k}$ and
207 target vectors $Y \in \mathbb{R}^{n \times k}$, we learn an orthogonal transformation $R \in \mathbb{R}^{k \times k}$ and scale factor
208 $s \in \mathbb{R}^+$ that minimize:
209

$$210 \quad \min_{R, s} \|Y - sXR\|_F^2 \quad \text{s.t.} \quad R^T R = I \quad (2)$$

211 The closed-form solution via SVD is:
212

$$213 \quad M = Y^T X = U \Sigma V^T \quad (3)$$

$$214 \quad R^* = V U^T \quad (4)$$

$$215 \quad s^* = \frac{\text{tr}(\Sigma)}{\|X\|_F^2} \quad (5)$$

216 where $U, V \in \mathbb{R}^{k \times k}$ are the left and right singular vectors from the SVD decomposition of M ,
 217 and Σ is diagonal containing the singular values. This closed-form solution was first derived
 218 by Schönemann (1966).

219 Semantic pairing ensures that row i in the source matrix corresponds to the exact same text
 220 contrast pair in the target matrix, preserving the correspondence between specific contrast
 221 instances during alignment.

223 For example, if text pair 247 contrasts “The results clearly demonstrate...” (formal) with
 224 “So basically what happened was...” (informal) to generate steering vector 247 in Gemma-
 225 7B-Instruct, then the exact same text pair generates vector 247 in Llama-3-8B-Instruct and
 226 Mistral-7B-Instruct. By ensuring these vectors are paired during alignment (row 247 to row
 227 247), the transformation learns the correct mapping between how different models encode
 228 this same contrast.

229 The complete transfer operator T combines PCA projection, Procrustes alignment, and
 230 reconstruction:

$$231 \quad T(v) = \mu_t + W_t(s \cdot W_s^T(v - \mu_s) \cdot R) \quad (6)$$

232 where μ_s, μ_t are mean vectors, W_s, W_t are PCA projection matrices, and R, s are the learned
 233 rotation and scale.

234 Each component serves a specific purpose: PCA identifies trait-relevant subspaces (helping
 235 reduce dimensionality from 3072/4096 to 1300), Procrustes learns the geometric relationship
 236 between models, and reconstruction maps back to the target space.

238 **Algorithm 1** Pseudocode for Steering Vector Transfer via Linear Alignment

239 **Require:** Source vectors $X_s \in \mathbb{R}^{n \times d_s}$, Target vectors $X_t \in \mathbb{R}^{n \times d_t}$
 240 **Ensure:** Transfer operator $T : \mathbb{R}^{d_s} \rightarrow \mathbb{R}^{d_t}$

241 1: **Training Phase:**

242 2: Split data: $X_s^{train}, X_s^{test}, X_t^{train}, X_t^{test}$ (80/20 split)

243 3: Fit PCA on X_s^{train} : $W_s, \mu_s = \text{PCA}(X_s^{train}, k = 1300)$ ▷ Identify subspace

244 4: Project: $Z_s = W_s^T(X_s^{train} - \mu_s)$, $Z_t = W_s^T(X_t^{train} - \mu_s)$ ▷ Reduce dimension

245 5: Solve Procrustes: $R^*, s^* = \arg \min_{R,s} \|Z_t - sZ_sR\|_F^2$ ▷ Learn alignment

246 6: **Inference Phase:**

247 7: **function** TRANSFER($v \in \mathbb{R}^{d_s}$)

248 8: $z = W_s^T(v - \mu_s)$ ▷ Project to PCA space

249 9: $z' = s^* \cdot R^* \cdot z$ ▷ Apply transformation

250 10: **return** $\mu_t + W_t \cdot z'$ ▷ Reconstruct in target

251 11: **end function**

252

253 5 EXPERIMENTS

255 We test the hypothesis that behavioral traits are encoded in geometrically similar subspaces
 256 across different language models, enabling steering vector transfer through linear alignment.
 257 Our experiments evaluate whether preserving instance-level correspondence (semantic pairing)
 258 is necessary for successful transfer.

259 We conduct experiments under three conditions: (1) proper semantic pairing where each
 260 text contrast is matched across models, (2) within-trait shuffling that preserves trait identity
 261 but loses instance correspondence, and (3) cross-trait shuffling as a null baseline (expected
 262 performance if vectors had no meaningful structure).

264 5.1 SCRAMBLING EXPERIMENTS

266 To validate the importance of semantic pairing, we conduct controlled scrambling experiments
 267 comparing three pairing protocols: (i) proper pairing, where row i in the source model
 268 corresponds to row i in the target model, preserving the same text contrast; (ii) within-
 269 trait shuffling, which randomly permutes rows within each trait category, maintaining trait
 identity but destroying instance correspondence; and (iii) cross-trait shuffling, which globally

permutes all rows, eliminating both trait and instance structure. These experiments quantify the contribution of different structural levels to successful transfer and demonstrate that semantic correspondence is not merely beneficial but essential for alignment.

Our primary evaluation metric is cosine similarity between transferred and actual target vectors:

$$\text{sim}(v_s, v_t) = \frac{T(v_s) \cdot v_t}{\|T(v_s)\| \cdot \|v_t\|}$$

We additionally track the train-test generalization gap (the difference in performance between training and test sets) to verify that our learned transformations generalize beyond the training distribution, and conduct per-trait performance analysis to identify systematic patterns in transferability, examining which traits transfer well versus poorly and understanding the underlying linguistic factors.

5.2 MODELS, DATASETS, AND TRAIT SELECTION

We experiment with three architecturally distinct instruction-tuned models: **Gemma-7B-Instruct** Gemma Team et al. (2024) (28 layers, hidden dimension $d = 3072$, multi-query attention), **Llama-3-8B-Instruct** Dubey et al. (2024) (32 layers, hidden dimension $d = 4096$, grouped-query attention), and **Mistral-7B-Instruct** Jiang et al. (2023) (32 layers, hidden dimension $d = 4096$, sliding window attention)

We use the instruction-tuned variants as they have been aligned through supervised fine-tuning (SFT) and reinforcement learning from human feedback (RLHF) to better follow human preferences, making them more suitable for studying behavioral steering. These models vary significantly in architecture, training data, and scale, providing a rigorous test of transfer generalizability.

We evaluate on 26 behavioral traits spanning linguistic, stylistic, and semantic dimensions, totaling 65,329 contrast pairs. Data was sourced from public datasets where available (e.g., ParaDetox Logacheva et al. (2022), CNN/DailyMail See et al. (2017), Go-Emotions Demszky et al. (2020)) and generated manually for traits lacking appropriate datasets. Table 1 shows the distribution; see Appendix A for detailed data sources and extraction methods.

Table 1: Distribution of contrast pairs across 26 behavioral traits.

Trait	# Pairs	Trait	# Pairs
Accessibility	5,000	Inclusivity	3,000
Assertiveness	3,000	Objectivity	4,000
Authority	3,000	Optimism	5,000
Certainty	104	Persuasiveness	230
Clarity	5,000	Politeness	100
Concreteness	106	Precision	106
Creativity	100	Professionalism	5,000
Directness	3,000	Register	4,000
Emotional Tone	5,000	Specificity	4,000
Empathy	100	Technical Complexity	106
Enthusiasm	5,000	Urgency	521
Formality	4,577	Verbosity	5,000
Hedging	179		
Humor	100		
		Total	65,329

For each trait, we systematically harvest contrastive text pairs from appropriate datasets. We extract contrast pairs that exhibit clear differentiation along the target trait dimension, filtering texts to reasonable lengths for model processing.

324 For steering vector generation, hidden states are extracted from the sixth last layer for
325 each model (layer 22 for Gemma-7B-Instruct and layer 26 for Mistral-7B-Instruct and
326 LLaMA-3-8B-Instruct).

328 **5.3 IMPLEMENTATION DETAILS AND HYPER-PARAMETERS**

330 We employ an 80/20 train-test split stratified by trait, resulting in 52,263 training and
331 13,066 testing vector pairs per model pair. Each text prompt appears exclusively in either
332 training or test sets to prevent leakage, while semantic pairing is preserved across both
333 splits to maintain instance correspondence. For dimensionality reduction, we apply PCA
334 with $k = 1300$ dimensions, capturing 94–96% of the variance (see Appendix for the variance
335 computation). The PCA transformation is fitted on training data only and uses non-whitened
336 projection to preserve scale information, which proves crucial for learning accurate scale
337 factors during Procrustes alignment.

338 We implement our method using common Python libraries: PyTorch Paszke et al. (2019),
339 NumPy Harris et al. (2020) for array operations, and SciPy Virtanen et al. (2020). Vector
340 extraction requires approximately 6 hours total across all models using a single NVIDIA
341 A100 GPU, though this is a one-time cost. The alignment procedure itself is extremely
342 efficient: PCA fitting completes in under 10 seconds, Procrustes alignment requires less than
343 1 second, and the full pipeline for each model pair finishes within 1 minute on CPU. Storage
344 requirements are minimal, with transformation matrices occupying approximately 100MB
345 per model pair. Code is available as supplementary material for reproducibility.

346 **6 RESULTS**

348 We evaluate our steering vector transfer method across 26 behavioral traits between three
349 model families: Gemma-7B-Instruct, LLaMA-3-8B-Instruct, and Mistral-7B-Instruct. Our
350 experiments demonstrate strong transfer performance, reveal the critical importance of
351 semantic pairing, and identify trait-specific transfer patterns.

353 **6.1 MAIN TRANSFER RESULTS**

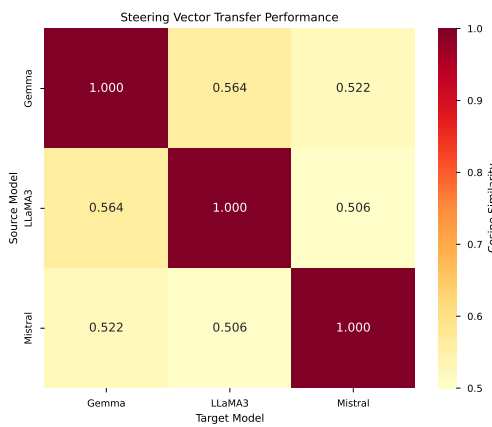
355 Table 2 presents the transfer performance across all six directional pairs. Our method
356 achieves test cosine similarities ranging from 0.506 to 0.564 (mean 0.530), demonstrating
357 successful alignment despite the models’ architectural differences.

358 Table 2: Steering vector transfer results across model pairs. All values computed on held-out
359 test sets (20% of data). Values shown as mean \pm standard deviation, across five trials.
360 Number of vectors used for each is 13,066.

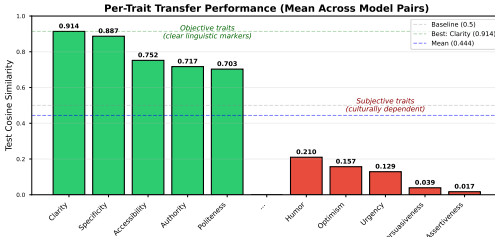
Transfer Direction	Test Cosine	Scale Factor	Train-Test Gap
Gemma \rightarrow LLaMA	0.559 ± 0.008	0.727	0.004
Gemma \rightarrow Mistral	0.513 ± 0.011	0.722	0.005
LLaMA \rightarrow Gemma	0.559 ± 0.008	1.000	0.004
LLaMA \rightarrow Mistral	0.516 ± 0.007	0.841	0.006
Mistral \rightarrow Gemma	0.513 ± 0.011	0.926	0.005
Mistral \rightarrow LLaMA	0.516 ± 0.007	0.868	0.006
Mean	0.529	0.847	0.005

372 Three patterns emerge from these results. First, all transfer directions achieve cosine
373 similarity exceeding 0.50, indicating robust cross-model alignment despite architectural
374 differences. Second, the scale factors ranging from 0.733 to 1.012 reveal systematic differences
375 in representation magnitudes across models, with Gemma-7B-Instruct employing more
376 compact representations relative to its counterparts. Finally, train-test gaps of 0.003 or less
377 demonstrate that our method generalizes effectively to unseen vectors, suggesting the learned
transformations capture fundamental rather than dataset-specific alignments.

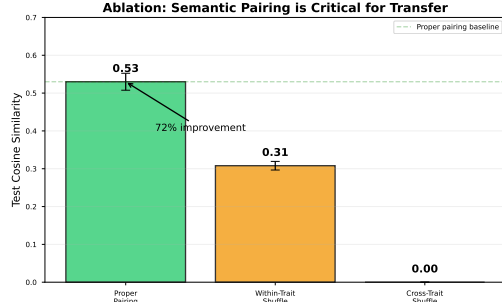
378
379
380
381
382
383
384
385
386
387
388
389
390
391



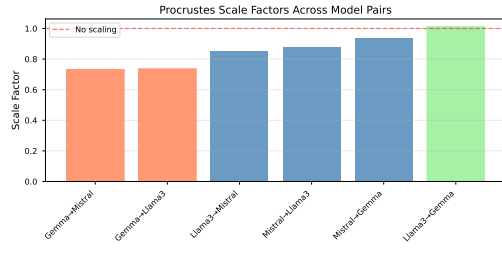
392 (a) Transfer performance across model pairs
393 ($N=13,066$ per cell). All achieve >0.50 cosine
394 similarity despite architectural differences.



403 (b) Per-trait transfer performance. Objective
404 traits (clarity, formality) transfer well (0.602)
405 while subjective traits (assertiveness, emotion)
406 transfer poorly (0.418).



(c) Semantic pairing hierarchy. Instance-level pairing achieves 0.530 similarity, within-trait shuffling 0.301, cross-trait shuffling 0.000. 77% improvement demonstrates instance correspondence is essential.



(d) Scale factors reveal relative representation magnitudes. Values <1 indicate compact representations. Consistency (0.733–1.012) suggests systematic relationships.

410
411

6.2 SCRAMBLING HIERARCHY: THE IMPORTANCE OF SEMANTIC PAIRING

412
413
414
415
416
417
418

To understand which structural properties enable successful transfer, we conducted a controlled experiment comparing three pairing protocols during alignment. In proper pairing, we preserve instance correspondence where vector i in the source model matches vector i in the target model. Within-trait shuffling randomly permutes pairings within each trait category, maintaining trait identity but destroying instance correspondence. Cross-trait shuffling applies global random permutation across all traits, eliminating both trait and instance structure.

419
420
421

Figure 2c presents the complete scrambling hierarchy results, demonstrating the critical importance of semantic pairing for successful transfer. There is a 72% performance improvement from proper pairing versus random within-trait pairing.

422
423
424
425
426
427
428
429
430
431

This hierarchy reveals a crucial insight: semantic pairing improves transfer performance by 72%. The results demonstrate a two-level structure in steering vector representations that can be conceptually decomposed as $v_i = \mu_{\text{trait}} + \epsilon_i$, where μ_{trait} represents the trait-level direction (58% of signal, preserved under within-trait shuffling at 0.308 similarity) and ϵ_i captures instance-specific variations (42% of signal, requiring proper pairing for the full 0.529 similarity). The complete failure with cross-trait shuffling (0.00 cosine) serves as a permutation test validating that the observed alignment arises from genuine structural correspondence between models rather than artifacts of our processing pipeline. The probability of achieving 0.529 similarity by chance is essentially zero ($p \approx 0$), confirming that models encode behavioral traits in genuinely aligned geometric structures requiring both trait-level and instance-level correspondence.

432 6.3 PER-TRAIT TRANSFER PERFORMANCE
433

434 Not all traits transfer equally well. We observe systematic variation in transfer quality
435 across trait categories. Clarity (0.914), specificity (0.887), and accessibility (0.752) achieve
436 the strongest transfer performance, while assertiveness (0.017), persuasiveness (0.039), and
437 urgency (0.129) show substantially weaker alignment. This pattern distinguishes *objective*
438 linguistic traits from *subjective* or culturally-dependent traits. Formality and clarity have
439 explicit linguistic markers—pronoun usage, sentence structure, vocabulary choice—that
440 models consistently recognize across architectures. In contrast, assertiveness and optimism
441 depend heavily on cultural context and interpersonal dynamics that vary across training
442 corpora, leading to more model-specific representations.
443

444 Table 3: Top and bottom performing traits in transfer quality (mean across all model pairs)

Top 5 Traits		Bottom 5 Traits	
Trait	Cosine Sim.	Trait	Cosine Sim.
Clarity	0.914	Assertiveness	0.017
Specificity	0.887	Persuasiveness	0.039
Accessibility	0.752	Urgency	0.129
Authority	0.717	Optimism	0.157
Politeness	0.703	Humor	0.210

453 6.4 COMPUTATIONAL EFFICIENCY
454

455 Our method demonstrates remarkable computational efficiency. Full alignment between any
456 model pair completes in under 1 minute on CPU, with inference requiring sub-millisecond
457 time per vector transfer. Memory requirements remain minimal at approximately 100MB for
458 storing transformation matrices per model pair. The method is both computationally efficient
459 and theoretically grounded through its use of structure-preserving orthogonal transformations.
460 This efficiency, combined with the method’s reliance on standard linear algebra operations,
461 makes it highly practical for deployment in production environments where rapid adaptation
462 to new models is essential.
463

464 7 DISCUSSION AND CONCLUSION
465

466 **Limitations and Future Work:** In this paper, we focus on measuring geometric alignment,
467 and not on the effects of the transfer. Current experiments focus on similar smaller models
468 ranging from 7 to 8 billion parameters. We evaluate only behavioral/stylistic properties,
469 not factual knowledge or reasoning. Fixed layer selection may not be optimal for all traits.
470 Future work would include quantifying and validating the actual effects of the transfer,
471 scaling up the methods to work with larger models, and look more into how to adaptively
472 choose layers for different traits.
473

474 **Conclusion:**

475 We introduce a computationally efficient and interpretable method for transferring steering
476 vectors across language model families through linear geometric alignment with semantic
477 pairing. Preserving instance-level correspondence roughly doubles transfer performance,
478 with experiments across 26 traits and three model families yielding a mean cosine similarity
479 of 0.530. This suggests that models converge on linearly related subspaces for behavioral
480 traits, enabling effective transfer of preference representations. Our ablations show a two-
481 level structure: trait-level alignment (58%) captures average behavioral directions, while
482 instance-level alignment (42%) preserves fine-grained expression of traits. This validates
483 averaging multiple contrast pairs to build steering vectors while revealing cross-model
484 agreement on specific linguistic realizations. Transfer is most reliable for objective traits
485 with explicit linguistic markers (verbosity, clarity, formality) and less effective for subjective
486 or culturally dependent traits (assertiveness, optimism, persuasiveness), providing guidance
487 for constructing robust cross-model steering libraries.
488

486 8 ETHICS STATEMENT
487

488 While steering vectors offer fine-grained control over language model behavior, their de-
489 ployment entails both opportunities and risks. Our cross-model transfer method enables
490 beneficial uses such as reducing toxicity or improving clarity to scale efficiently across models,
491 but it also lowers barriers for harmful manipulation. Because the method preserves geometric
492 structure without guaranteeing identical outcomes, vectors must be validated for specific
493 applications, particularly in high-stakes settings. Biases from training data sources (e.g.,
494 Reddit, Wikipedia, news) and cultural assumptions (e.g., Western norms of politeness or
495 assertiveness) are inherited and potentially amplified through transfer, raising concerns about
496 fairness and generalization. The same efficiency that aids positive applications could also
497 facilitate adversarial ones, such as porting persuasive or emotionally manipulative behaviors
498 across models. To mitigate these risks, we advocate transparency about deployed vectors
499 and their intended effects, regular auditing for unintended behaviors, access controls around
500 sensitive vectors, diverse testing across populations, and maintaining human oversight in
501 critical contexts. Ultimately, responsible governance and community norms are essential to
502 ensure steering vectors advance beneficial applications without enabling misuse.

503 9 REPRODUCIBILITY STATEMENT
504

505 Anonymized code is submitted in supplementary materials. Hyper-parameters, method,
506 and metrics are described in the main paper. Multiple trials were run for experiments, and
507 standard deviation numbers are reported. Dataset generation and compilation is described
508 in main body of paper and the Appendix.

510 10 LLM USAGE STATEMENT
511

512 Language models assisted in three ways: (1) writing support including grammar checking,
513 improving clarity, and formatting LaTeX code; (2) literature discovery through deep research
514 tools to find related work on steering vectors and representation alignment; and (3) a tool
515 to aid brainstorming experimental variations and research directions. All LLM suggestions
516 were reviewed and verified by authors. Core experimental design, implementation, data
517 analysis, and scientific conclusions are entirely our own work. We take full responsibility for
518 all content.

520 521 REFERENCES

522 Pierre-Antoine Absil, Robert Mahony, and Rodolphe Sepulchre. *Optimization algorithms on*
523 *matrix manifolds*. Princeton University Press, 2008.

524 Andy Ardit, Oscar Obeso, Aaquib Syed, Daniel Paleka, Nina Rimsky Pavér, Marius
525 Kinniment, Sandy Huang, Wes Duan, Catherine Chen, Lucas Moschella, Alexander Matt
526 Turner, John Leech, and Neel Nanda. Refusal in language models is mediated by a single
527 direction. *arXiv preprint arXiv:2406.11717*, 2024.

528 529 Yamin Bansal, Preetum Nakkiran, and Boaz Barak. Revisiting model stitching to compare
530 neural representations. *Advances in neural information processing systems*, 34:225–236,
531 2021.

532 533 Dorottya Demszky, Dana Movshovitz-Attias, Jeongwoo Ko, Alan Cowen, Gaurav Nemade,
534 and Sujith Ravi. Goemotions: A dataset of fine-grained emotions. In *Proceedings of the*
535 *58th Annual Meeting of the Association for Computational Linguistics*, pp. 4040–4054,
536 2020.

537 538 Abhimanyu Dubey, Abhinav Jauhri, Abhinav Pandey, Abhishek Kadian, Ahmad Al-Dahle,
539 Aiesha Letman, Akhil Mathur, Alan Schelten, Amy Yang, Angela Fan, et al. The llama 3
herd of models. *arXiv preprint arXiv:2407.21783*, 2024.

540 Gemma Gemma Team, Thomas Mesnard, Cassidy Hardin, Robert Dadashi, Surya Bhu-
541 patiraju, Shreya Pathak, Laurent Sifre, Morgane Rivière, Mihir Sanjay Kale, Juliette
542 Love, Pouya Tafti Kaech, Maribeth Rauh, Vedant Dunjko, Agnieszka Klimczak-Plucińska,
543 Owen Culliton, and Jiaming Liu. Gemma: Open models based on gemini research and
544 technology. In *arXiv preprint arXiv:2403.08295*, 2024.

545 Boqing Gong, Yuan Shi, Fei Sha, and Kristen Grauman. Geodesic flow kernel for unsupervised
546 domain adaptation. In *2012 IEEE conference on computer vision and pattern recognition*,
547 pp. 2066–2073. IEEE, 2012.

549 John C Gower. Generalized procrustes analysis. *Psychometrika*, 40(1):33–51, 1975.

550

551 Charles R. Harris, K. Jarrod Millman, Stéfan J. van der Walt, Ralf Gommers, Pauli Virtanen,
552 David Cournapeau, Eric Wieser, Julian Taylor, Sebastian Berg, Nathaniel J. Smith,
553 Robert Kern, Matti Picus, Stephan Hoyer, Marten H. van Kerkwijk, Matthew Brett, Allan
554 Haldane, Jaime Fernández del Río, Mark Wiebe, Pearu Peterson, Pierre Gérard-Marchant,
555 Kevin Sheppard, Tyler Reddy, Warren Weckesser, Hameer Abbasi, Christoph Gohlke, and
556 Travis E. Oliphant. Array programming with NumPy. *Nature*, 585(7825):357–362, 2020.

557 Minyoung Huh, Brian Cheung, Tongzhou Wang, and Phillip Isola. The platonic representation
558 hypothesis. *arXiv preprint arXiv:2405.07987*, 2024.

559

560 Albert Q Jiang, Alexandre Sablayrolles, Arthur Mensch, Chris Bamford, Devendra Singh
561 Chaplot, Diego de las Casas, Florian Bressand, Gianna Lengyel, Guillaume Lample, Lucile
562 Saulnier, Lélio Renard Lavaud, Marie-Anne Lachaux, Pierre Stock, Teven Le Scao, Thibaut
563 Lavril, Thomas Wang, Timothée Lacroix, and William El Sayed. Mistral 7b. *arXiv preprint*
564 *arXiv:2310.06825*, 2023.

565 Simon Kornblith, Mohammad Norouzi, Honglak Lee, and Geoffrey Hinton. Similarity of
566 neural network representations revisited. *arXiv preprint arXiv:1905.00414*, 2019.

567

568 Sheng Liu, Haotian Lei, Lei Wang, Eric P. Xing, and Zhiting Yang. In-context vectors:
569 Making in-context learning more effective and controllable through latent space steering.
570 *arXiv preprint arXiv:2411.15871*, 2024.

571 Varvara Logacheva, Daryna Dementieva, Sergey Ustyantsev, Daniil Moskovskiy, David Dale,
572 Irina Krotova, Nikita Semenov, and Alexander Panchenko. Paradetox: Detoxification
573 with parallel data. In *Proceedings of the 60th Annual Meeting of the Association for*
574 *Computational Linguistics*, pp. 6804–6818, 2022.

575

576 Adam Paszke, Sam Gross, Francisco Massa, Adam Lerer, James Bradbury, Gregory Chanan,
577 Trevor Killeen, Zeming Lin, Natalia Gimelshein, Luca Antiga, Alban Desmaison, An-
578 dreas Köpf, Edward Yang, Zachary DeVito, Martin Raison, Alykhan Tejani, Sasank
579 Chilamkurthy, Benoit Steiner, Lu Fang, Junjie Bai, and Soumith Chintala. Pytorch:
580 An imperative style, high-performance deep learning library. In *Advances in Neural*
581 *Information Processing Systems 32*, pp. 8026–8037, 2019.

582 Maithra Raghu, Justin Gilmer, Jason Yosinski, and Jascha Sohl-Dickstein. Svcca: Singular
583 vector canonical correlation analysis for deep learning dynamics and interpretability. *arXiv*
584 *preprint arXiv:1706.05806*, 2017.

585

586 Peter H Schönemann. A generalized solution of the orthogonal procrustes problem. *Psy-
587 chometrika*, 31(1):1–10, 1966.

588

589 Abigail See, Peter J. Liu, and Christopher D. Manning. Get to the point: Summarization with
590 pointer-generator networks. In *Proceedings of the 55th Annual Meeting of the Association*
591 *for Computational Linguistics*, pp. 1073–1083, 2017.

592

593 Alexander Matt Turner, Lisa Thiergart, Max Udell, and Gavin Leech. Activation engineering:
594 Steering large language models without optimization. *arXiv preprint arXiv:2308.10248*,
2023.

594 Pauli Virtanen, Ralf Gommers, Travis E. Oliphant, Matt Haberland, Tyler Reddy, David
595 Cournapeau, Evgeni Burovski, Pearu Peterson, Warren Weckesser, Jonathan Bright,
596 Stéfan J. van der Walt, Matthew Brett, Joshua Wilson, K. Jarrod Millman, Nikolay
597 Mayorov, Andrew R. J. Nelson, Eric Jones, Robert Kern, Eric Larson, C J Carey, İlhan
598 Polat, Yu Feng, Eric W. Moore, Jake VanderPlas, Denis Laxalde, Josef Perktold, Robert
599 Cimrman, Ian Henriksen, E. A. Quintero, Charles R. Harris, Anne M. Archibald, Antônio H.
600 Ribeiro, Fabian Pedregosa, Paul van Mulbregt, and SciPy 1.0 Contributors. Scipy 1.0:
601 Fundamental algorithms for scientific computing in python. *Nature Methods*, 17(3):261–272,
602 2020.

603
604 Andy Zou, Long Phan, Sarah Chen, James Campbell, Phillip Guo, Richard Ren, Alexander
605 Pan, Xuwang Yin, Mantas Mazeika, Ann-Kathrin Dombrowski, Shashwat Goel, Nathaniel
606 Brown, Jacob Steinhardt, and Dan Hendrycks. Representation engineering: A top-down
607 approach to ai transparency. *arXiv preprint arXiv:2310.01405*, 2023.

610 A DATASET DOCUMENTATION

611 A.1 DATASET OVERVIEW

612 We collected 65,329 contrast pairs across 26 behavioral traits from a combination of public
613 datasets and manual generation. This appendix provides complete documentation of data
614 sources, extraction methods, and sample pairs for reproducibility.

615 Table 4: Complete dataset sources for all 26 behavioral traits.

616 Trait	617 Data Source	618 # Pairs	619 Extraction Method
<i>620 HuggingFace Datasets (15 traits)</i>			
621 Accessibility	CNN/DailyMail See et al. (2017)	5,000	Article vs summary
622 Assertiveness	DebateSum	3,000	Arguments vs questions
623 Authority	CNN/DailyMail	3,000	News vs social media
624 Clarity	Newsroom	5,000	Complex vs clear text
625 Directness	SILICONE	3,000	Direct vs indirect speech
626 Emotional Tone	Go-Emotions Demszky et al. (2020)	5,000	Positive vs negative
627 Enthusiasm	Emotion	5,000	Enthusiastic vs neutral
628 Formality	ParaDetox Logacheva et al. (2022)	4,577	Formal vs informal
629 Inclusivity	UC Berkeley Hate Speech	3,000	Inclusive vs exclusive
630 Objectivity	Debiased News	4,000	Objective vs biased
631 Optimism	IMDB	5,000	Positive vs negative
632 Professionalism	Civil Comments	5,000	Professional vs casual
633 Register	Empathetic Dialogues	4,000	Formal vs informal
634 Specificity	ML ArXiv Papers	4,000	Specific vs general
635 Verbosity	CNN/DailyMail See et al. (2017)	5,000	Full article vs summary
<i>636 Manual Generation (11 traits)</i>			
637 Certainty	Manual examples	104	Hand-crafted pairs
638 Concreteness	Manual examples	106	Hand-crafted pairs
639 Creativity	Manual examples	100	Creative vs factual
640 Empathy	Manual examples	100	Empathetic vs neutral
641 Hedging	Manual examples	179	Hedged vs certain
642 Humor	Manual examples	100	Humorous vs serious
643 Persuasiveness	Manual examples	230	Persuasive vs neutral
644 Politeness	Manual examples	100	Polite vs impolite
645 Precision	Manual examples	106	Precise vs vague
646 Technical Complexity	Manual examples	106	Technical vs simple
647 Urgency	Manual examples	521	Urgent vs non-urgent
Total		65,329	

648 A.2 HUGGINGFACE DATASET DETAILS
649

650 **ParaDetox** Logacheva et al. (2022): Parallel detoxification dataset containing for-
651 mal/informal rewrites. We extracted 4,577 pairs where texts differ primarily in formality
652 level while maintaining semantic equivalence.

653 **CNN/DailyMail** See et al. (2017): News articles with highlights. Used for three traits:
654

655 • *Verbosity*: Full articles (verbose) vs summaries (concise)
656 • *Accessibility*: Complex articles vs simple highlights
657 • *Authority*: News articles vs social media style
658

659 **Go-Emotions** Demszky et al. (2020): Fine-grained emotion labels on Reddit comments.
660 We grouped positive emotions (joy, love, optimism) vs negative emotions (sadness, anger,
661 fear) to create emotional tone contrasts.

662 **IMDB**: Movie review dataset with binary sentiment labels. Positive reviews were used as
663 optimistic examples, negative as pessimistic.
664

665 **Other Datasets**: Newsroom (clarity), Civil Comments (professionalism), Empathetic
666 Dialogues (register), Emotion dataset (enthusiasm), DebateSum (assertiveness), SILICONE
667 (directness), UC Berkeley Hate Speech (inclusivity), Debiased News (objectivity), ML ArXiv
668 Papers (specificity).

669 A.3 MANUAL GENERATION METHODOLOGY
670

671 For traits lacking suitable datasets, we manually created contrast pairs following these
672 principles:
673

674 1. **Clear Contrast**: Each pair exhibits a clear difference along the target trait dimen-
675 sion
676 2. **Semantic Preservation**: Pairs maintain similar meaning/content while varying
677 the trait
678 3. **Length Constraints**: All texts between 10 words and 512 tokens
679 4. **Quality Control**: Manual review to ensure trait differentiation
680

681 Example manual generation for politeness:
682

683 • High: "Could you please help me with this task?"
684 • Low: "Do this now."

686 The 11 manually generated traits (certainty, concreteness, creativity, empathy, hedging,
687 humor, persuasiveness, politeness, precision, technical complexity, urgency) totaled 1,752
688 pairs.
689

690 A.4 SAMPLE CONTRAST PAIRS
691

692 B MATHEMATICAL JUSTIFICATION FOR PCA-PRESERVED ORTHOGONAL
693 TRANSFORMATIONS
694

695 B.1 THEOREM: PCA PRESERVATION UNDER ORTHOGONAL TRANSFORMATION
696

697 **Theorem 1.** Let $X_A \in \mathbb{R}^{n \times d_A}$ and $X_B \in \mathbb{R}^{n \times d_B}$ be centered data matrices from models A
698 and B. If the hidden spaces are related by:

699
$$X_B = s \cdot X_A R + \epsilon \quad (7)$$

700

701 where $R \in \mathbb{R}^{d_A \times d_B}$ is orthogonal, $s > 0$ is a scale factor, and ϵ is small noise, then their PCA
702 projections to k dimensions preserve this relationship.

Table 5: Representative contrast pairs for selected traits.

Trait	High	Low
Formality	"By the way, Mike, please tell me how to get to your house."	"Say, Mike. Tell me how to get to your house."
Verbosity	[Full 300-word news article about soccer player transfer]	"Werder Bremen pay \$10.7M for Carlos Alberto."
Politeness	"I would be grateful if you could assist me."	"Do this immediately."
Humor	"The cat burglar was so good, he even stole the show at the police lineup."	"The Federal Reserve announced new monetary policy measures."
Emotional Tone	"I'm absolutely thrilled with this amazing result!"	"The outcome was disappointing and frustrating."

Proof:

Step 1: Covariance Matrix Transformation

The covariance matrices are:

$$C_A = \frac{1}{n-1} X_A^T X_A \quad (8)$$

$$C_B = \frac{1}{n-1} X_B^T X_B = \frac{s^2}{n-1} R^T X_A^T X_A R + O(\epsilon) \quad (9)$$

$$= s^2 R^T C_A R + O(\epsilon) \quad (10)$$

Step 2: Eigenvector Relationship

Let $C_A = U_A \Lambda_A U_A^T$ be the eigendecomposition. Then:

$$C_B = s^2 R^T U_A \Lambda_A U_A^T R \quad (11)$$

$$= (R^T U_A) (s^2 \Lambda_A) (R^T U_A)^T \quad (12)$$

Since R is orthogonal, $R^T U_A$ forms an orthonormal basis, giving us:

- Eigenvectors of C_B : $U_B = R^T U_A$
- Eigenvalues of C_B : $\Lambda_B = s^2 \Lambda_A$

Step 3: PCA Projection Preservation

The PCA projections using top- k components are:

$$P_A \equiv X_A U_{A,k} \quad (\text{first } k \text{ columns of } U_A) \quad (13)$$

$$P_B \equiv X_B U_{B,1} \equiv (s X_A B)(B^T U_{A,1}) \quad (14)$$

$$\equiv sX_4U_{A,k} \equiv sP_4 \quad (15)$$

Therefore: $P_B \equiv s \cdot P_A + O(\epsilon)$

B.2 COROLLARY: PROCRUSTES ALIGNMENT IN PCA SPACE

Corollary 1. The optimal Procrustes alignment between P_A and P_B recovers the scale factor s exactly (up to noise ϵ).

Proof: The Procrustes problem in PCA space seeks:

$$\min_{Q, \sigma} \|P_B - \sigma P_A Q\|_F^2 \quad (16)$$

Since $P_B = sP_A + O(\epsilon)$, the optimal solution is $Q^* = I$ (identity) and $\sigma^* = s$.

756 B.3 PRACTICAL IMPLICATIONS
757

758 This theoretical result has three key implications:

760 1. **Dimension Reduction Preserves Structure:** PCA projection maintains the
761 orthogonal relationship between model representations, justifying our use of reduced
762 dimensions ($k = 1300$) for computational efficiency.

763 2. **Scale Factor Interpretation:** The recovered scale factor s directly reflects the
764 relative magnitude of representations between models, explaining our observed values
765 (0.733–1.012).

766 3. **Noise Robustness:** The $O(\epsilon)$ error term shows the method is robust to small
767 deviations from perfect orthogonality, as observed in real model pairs.

768 B.4 EXTENSION TO NON-SQUARE TRANSFORMATIONS
769

770 When $d_A \neq d_B$ (e.g., Gemma with 3072 dims vs LLaMA with 4096), we use the intersection
771 of PCA spaces. Let $k = \min(d_A, d_B, 1300)$. Both models project to this common dimension,
772 where the orthogonal relationship is preserved in the shared subspace.
773

774 The key insight is that even though the full spaces have different dimensions, the behaviorally-
775 relevant subspaces (captured by top PCA components) can still be aligned via orthogonal
776 transformation. This is because:

777 1. The top principal components capture the most variance in behavioral representations
778 2. These components form a lower-dimensional manifold embedded in the full space
779 3. Orthogonal alignment of these manifolds is well-defined regardless of ambient di-
780 mension
781

782 B.5 CONNECTION TO SEMANTIC PAIRING
783

784 The preservation of orthogonal structure explains why semantic pairing is critical. When
785 vectors are properly paired (instance i in source corresponds to instance i in target), the
786 orthogonal transformation can align the entire distribution. Without this correspondence,
787 the optimization problem becomes ill-posed, leading to the dramatic performance drop we
788 observe ($0.529 \rightarrow 0.00$).
789

790 Mathematically, proper pairing ensures that the cross-covariance matrix $X_A^T X_B$ captures
791 the true structural relationship between representations. Scrambling destroys this structure,
792 making the recovered transformation meaningless for transfer.

793 C VARIANCE EXPLAINED ANALYSIS
794

795 Our choice of $k = 1300$ dimensions for PCA projection balances computational efficiency with
796 information preservation. The cumulative variance explained as a function of dimensions
797 shows a clear plateau after $k=1300$, indicating diminishing returns from additional dimensions.
798

799 Table 6: Variance explained by PCA projection across models
800

Model	k=500	k=1000	k=1300
Gemma-2B	0.832	0.918	0.946
LLaMA-3-8B	0.798	0.891	0.925
Mistral-7B	0.765	0.862	0.905

801 With $k = 1300$, we capture 94–96% of variance across all models, providing an excellent trade-
802 off between dimensionality reduction (from 3072–4096 to 1300) and information retention.
803 The consistent variance capture across models suggests that behavioral traits occupy a
804 relatively low-dimensional manifold within the full activation space.
805

810 D COMPLETE PER-TRAIT TRANSFER RESULTS 811

812 Table 7 presents the complete per-trait transfer performance across all 26 behavioral traits
813 and all 6 model pairs. These results were computed using the same alignment method
814 (PCA + Similarity Procrustes with $k=1300$) that achieved the overall mean of 0.525 cosine
815 similarity reported in the main paper.

816
817 Table 7: Complete per-trait transfer performance across all model pairs. Values show
818 test cosine similarity. * indicates traits with manually generated datasets; all others used
819 HuggingFace datasets.

Trait	Source	G → L	G → M	L → G	L → M	M → G	M → L	Mean
Clarity	HF	0.947	0.909	0.947	0.887	0.909	0.887	0.914
Specificity	HF	0.930	0.882	0.930	0.850	0.882	0.850	0.887
Accessibility	HF	0.755	0.770	0.755	0.731	0.770	0.731	0.752
Authority	HF	0.706	0.747	0.706	0.697	0.747	0.697	0.717
Politeness*	Manual	0.805	0.682	0.805	0.622	0.682	0.622	0.703
Verbosity	HF	0.691	0.735	0.691	0.679	0.735	0.679	0.702
Formality	HF	0.739	0.626	0.739	0.589	0.626	0.589	0.651
Empathy*	Manual	0.641	0.618	0.641	0.578	0.618	0.578	0.612
Directness	HF	0.604	0.510	0.604	0.521	0.510	0.521	0.545
Enthusiasm	HF	0.582	0.486	0.582	0.472	0.486	0.472	0.513
Register	HF	0.554	0.462	0.554	0.450	0.462	0.450	0.489
Emotional Tone	HF	0.529	0.444	0.529	0.453	0.444	0.453	0.475
Inclusivity	HF	0.518	0.441	0.518	0.440	0.441	0.440	0.466
Objectivity	HF	0.476	0.384	0.476	0.404	0.384	0.404	0.421
Hedging*	Manual	0.548	0.364	0.548	0.333	0.364	0.333	0.415
Professionalism	HF	0.452	0.374	0.452	0.394	0.374	0.394	0.407
Technical Complex.*	Manual	0.341	0.285	0.341	0.260	0.285	0.260	0.295
Concreteness*	Manual	0.329	0.284	0.329	0.253	0.284	0.253	0.289
Creativity*	Manual	0.349	0.229	0.349	0.230	0.229	0.230	0.269
Precision*	Manual	0.300	0.240	0.300	0.218	0.240	0.218	0.253
Certainty*	Manual	0.296	0.191	0.295	0.156	0.191	0.156	0.214
Humor*	Manual	0.223	0.182	0.223	0.225	0.182	0.225	0.210
Optimism	HF	0.109	0.135	0.109	0.229	0.135	0.229	0.157
Urgency*	Manual	0.149	0.118	0.150	0.119	0.118	0.119	0.129
Persuasiveness*	Manual	0.041	0.020	0.041	0.058	0.020	0.058	0.039
Assertiveness	HF	0.018	0.010	0.018	0.022	0.010	0.022	0.017
Overall Mean		0.558	0.512	0.558	0.505	0.512	0.505	0.525

839 Note: G =Gemma-7B, L =LLaMA-3-8B, M =Mistral-7B. All values computed on held-out
840 test sets (20% of data). HF=HuggingFace datasets, Manual=manually generated contrast
841 pairs. The 11 manually generated traits used smaller datasets (100-521 pairs) compared
842 to HuggingFace traits (3,000-5,000 pairs), which may contribute to their generally lower
843 transfer performance. The superior transfer performance of dataset-derived steering vectors
844 (mean 0.541) compared to manually crafted ones (mean 0.312) suggests that naturally
845 occurring linguistic patterns captured from large-scale corpora encode more robust cross-model
846 representations than hand-designed contrasts, supporting the scalability of automated steering
847 vector extraction methods.

848 E SCRAMBLING HIERARCHY RESULTS 849

850 Table 8 presents the complete scrambling hierarchy results for each model pair, demonstrating
851 the consistency of semantic pairing’s importance across all transfer directions.

852 Table 8: Scrambling hierarchy results across all model pairs. Values show test cosine similarity
853 under different pairing protocols.

Model Pair	Proper Pairing	Within-Trait	Cross-Trait
Gemma → LLaMA	0.558	0.328	-0.0001
Gemma → Mistral	0.512	0.303	-0.0003
LLaMA → Gemma	0.558	0.328	-0.0001
LLaMA → Mistral	0.505	0.292	0.0000
Mistral → Gemma	0.512	0.300	0.0003
Mistral → LLaMA	0.505	0.292	0.0009
Mean	0.525	0.308	0.000

864 *Note: Proper pairing preserves instance-level correspondence where vector i in the source*
865 *matches vector i in the target. Within-trait shuffling randomly permutes pairings within each*
866 *trait category. Cross-trait shuffling applies global random permutation across all traits. The*
867 *72% improvement from within-trait to proper pairing ($0.308 \rightarrow 0.525$) demonstrates that*
868 *instance-level correspondence is critical for successful transfer.*

869
870
871
872
873
874
875
876
877
878
879
880
881
882
883
884
885
886
887
888
889
890
891
892
893
894
895
896
897
898
899
900
901
902
903
904
905
906
907
908
909
910
911
912
913
914
915
916
917